PHYSICAL REVIEW D **85,** 074012 (2012)

Quark-lepton symmetric model at the LHC

Jackson D. Clarke, Robert Foot, and Raymond R. Volkas

ARC Centre of Excellence for Particle Physics at the Terascale School of Physics, University of Melbourne, 3010, Australia

(Received 14 December 2011; published 10 April 2012)

We investigate the quark-lepton symmetric model of Foot and Lew in the context of the Large Hadron Collider (LHC). In this ''bottom-up'' extension to the standard model, quark-lepton symmetry is achieved by introducing a gauged ''leptonic color'' symmetry which is spontaneously broken above the electroweak scale. If this breaking occurs at the TeV scale, then we expect new physics to be discovered at the LHC. We examine three areas of interest: the Z' heavy neutral gauge boson, charge $\pm 1/2$ exotic leptons, and a color triplet scalar diquark. We find that the LHC has already explored and/or will explore new parameter space for these particles over the course of its lifetime.

DOI: 10.1103/PhysRevD.85.074012 PACS numbers: 13.85.Rm, 12.60.Cn, 13.85.Qk

I. INTRODUCTION

The Large Hadron Collider (LHC) has begun probing physics at the TeV scale. The goals are to discover the origin of electroweak symmetry breaking and to search for new physics. The purpose of this paper is to analyze the LHC phenomenology of the discrete quark-lepton (q-l) symmetric model of Foot and Lew [1]. This theory is conceptually related to both the Pati-Salam model [2] and the left-right symmetric model [3]. Like the Pati-Salam model, it unifies the quantum numbers of the leptons with those of the quarks, but it does so using a discrete exchange symmetry rather than a continuous symmetry. This discrete symmetry can be viewed as the quark/lepton analogue of the discrete (parity or charge-conjugation) symmetry used in the left-right symmetric model to unify the quantum numbers of left-handed fermions with their right-handed partners. The q-l symmetric model is distinct from grand unification, because it does not require the concomitant unification of the strong and electroweak interactions.[1] The absence of a continuous symmetry transforming quarks into leptons and vice-versa allows the scale of the new physics to be as low as a TeV, making it testable at the LHC.

We now review how the q-l symmetric model incorporates a discrete symmetry between quarks and leptons. Under the standard model (SM) gauge group,

$$G_{\rm SM} = SU(3)_q \times SU(2)_L \times U(1)_Y, \tag{1}$$

quarks and leptons transform as

$$\begin{aligned} Q_L &\sim (3,2)(1/3), & f_L &\sim (1,2)(-1), \\ u_R &\sim (3,1)(4/3), & e_R &\sim (1,1)(-2), \\ d_R &\sim (3,1)(-2/3), & \nu_R &\sim (1,1)(0), \end{aligned} \tag{2}$$

where we have included a right-handed neutrino for neutrino mass generation purposes. Some similarities between quarks and leptons are immediately obvious. They are both fermions in three generations and each sector transforms as $2 \oplus 1 \oplus 1$ under $\mathrm{SU}(2)_L$. However, as is self-evident, quarks have a color charge under $\mathrm{SU}(3)_q$ while leptons do not, and the hypercharges are different.

One can increase quark-lepton symmetry by introducing a ''leptonic color'' gauge interaction through an independent SU(3) group. The SM gauge group is enlarged to

$$G_{ql} = SU(3)_l \times SU(3)_q \times SU(2)_L \times U(1)_X, \tag{3}$$

where $\mathrm{SU}(3)_l$ is the new leptonic color group and X is a charge described in Sec. II. The number of leptons is tripled, and $\mathrm{SU}(3)_l$ must be spontaneously broken. This is achieved through one or more scalar multiplets that carry leptonic color acquiring nonzero vacuum expectation values (VEVs).

After this breaking, the SM is recovered as a low-energy effective theory. The breaking pattern is

$$\begin{array}{c} SU(3)_l \times SU(3)_q \times SU(2)_L \times U(1)_X \\ \downarrow w \\ SU(2)' \times SU(3)_q \times SU(2)_L \times U(1)_Y \\ \downarrow u \\ SU(2)' \times SU(3)_q \times U(1)_Q, \end{array} \tag{4}$$

where w and u are the breaking scales, Q is electric charge and $\mathrm{SU}(2)'$ remains as an unbroken remnant of $\mathrm{SU}(3)_l$. This $\mathrm{SU}(2)'$ group is asymptotically free and expected to be confining. Since all particles in nontrivial $\mathrm{SU}(2)'$ representations are very massive (see below), the low-energy limit is indeed the SM despite this additional gauge force.

This paper is structured as follows: Section II is an overview of the construction of the q-l symmetric model. We then move on to a study of phenomenology at the LHC. In Sec. III, we look at a heavy neutral gauge boson called Z'. We use LHC data to put a lower bound on the mass of this particle. In Sec. IV, we investigate the charge $\pm 1/2$ exotic leptons which gain a large mass at the leptonic color

[1] It is, however, compatible with an eventual high-scale grand unification, through a structure now known as ''quartification'' [4].

breaking scale. We show that the LHC will explore new parameter space for these particles in the near future. In Sec. V, we look at a color triplet scalar diquark. Using Tevatron and LHC data we constrain mass-coupling parameter space for this diquark. Section VI contains the conclusion.

II. QUARK-LEPTON SYMMETRIC MODEL

We consider the q-l symmetric model constructed in Ref. [5]. When the SM gauge group is enlarged as in Eq. (3), we write the quark-lepton spectrum as

$$\begin{aligned} &Q_L \sim (1,3,2)(1/3), && F_L \sim (3,1,2)(-1/3), \\ &u_R \sim (1,3,1)(4/3), && E_R \sim (3,1,1)(-4/3), \\ &d_R \sim (1,3,1)(-2/3), && N_R \sim (3,1,1)(2/3). \end{aligned} \tag{5}$$

The leptonic components can be expressed as

$$F_L = \begin{pmatrix} f_L \\ F_{1L} \\ F_{2L} \end{pmatrix}, \quad E_R = \begin{pmatrix} e_R \\ E_{1R} \\ E_{2R} \end{pmatrix}, \quad N_R = \begin{pmatrix} \nu_R \\ V_{1R} \\ V_{2R} \end{pmatrix}, \tag{6}$$

where f_L, e_R, ν_R are the familiar SM leptons and right-handed neutrino, and F_{iL}, E_{iR}, V_{iR} $(i = 1, 2)$ are the exotic fermions named "liptons." The generational indices are suppressed. The components of F_L are each doublets under $\mathrm{SU}(2)_L$:

$$f_L = \begin{pmatrix} \nu_L \\ e_L \end{pmatrix}, \qquad F_{iL} = \begin{pmatrix} V_{iL} \\ E_{iL} \end{pmatrix}. \tag{7}$$

The simplest way to achieve electroweak symmetry breaking is through a Higgs doublet, $\phi \sim (1,1,2)(1)$, analogously to the SM. The simplest Yukawa Lagrangian,

$$\begin{aligned} \mathcal{L}^{(1)}_{Yuk} = {} & \lambda_1[\bar{F}_L E_R \phi + \bar{Q}_L u_R \phi^c] \\ & + \lambda_2[\bar{F}_L N_R \phi^c + \bar{Q}_L d_R \phi] + \text{H.c.}, \end{aligned} \tag{8}$$

where $\phi^c \equiv i\tau_2 \phi^*$ and τ_2 is the second Pauli matrix, leads to unacceptable tree-level mass relations between quarks and leptons. These relations are easily avoided by instead introducing two Higgs doublets, ϕ_1 and ϕ_2, as described in Ref. [6].

Leptonic color symmetry breaking is achieved by introducing the Higgs triplets $\chi_1 \sim (3,1,1)(2/3)$ and $\chi_2 \sim (1,3,1)(-2/3)$ through the Yukawa Lagrangian

$$\begin{aligned} \mathcal{L}^{(2)}_{Yuk} = {} & h_1[\overline{(F_L)^c} F_L \chi_1 + \overline{(Q_L)^c} Q_L \chi_2] \\ & + h_2[\overline{(E_R)^c} N_R \chi_1 + \overline{(u_R)^c} d_R \chi_2] + \text{H.c.} \end{aligned} \tag{9}$$

The leptonic color symmetry is broken by a nonzero VEV for χ_1. It induces the breaking

$$SU(3)_l \times U(1)_X \to SU(2)' \times U(1)_Y, \tag{10}$$

where

$$Y = X + \frac{1}{3}T \tag{11}$$

and $T = \mathrm{diag}(-2,1,1)$. The χ_1 VEV also generates masses for the liptons.

One can generate small ν masses in a number of ways, for example, by inducing a seesaw mechanism through Higgs multiplets $\Delta_1 \sim (\bar{6},1,1)(-4/3)$ and $\Delta_2 \sim (1,\bar{6},1)(4/3)$ as in Refs. [5,6], through additional Higgs doublets [6], or via additional singlet fermions [7].

One can now see that a Z_2 discrete symmetry of the Lagrangian

$$\begin{aligned} &Q_L \leftrightarrow F_L, && \chi_1 \leftrightarrow \chi_2, && G^\mu_q \leftrightarrow G^\mu_l, \\ &u_R \leftrightarrow E_R, && \phi \leftrightarrow \phi^c, && C^\mu \leftrightarrow -C^\mu, \\ &d_R \leftrightarrow N_R, \end{aligned} \tag{12}$$

can be postulated, where $G^\mu_{q,l}$ are the gauge bosons of $\mathrm{SU}(3)_{q,l}$ and C^μ is the gauge boson of $\mathrm{U}(1)_X$. This is the quark-lepton symmetry.

III. THE Z′ NEUTRAL GAUGE BOSON

A. Coupling

Like many extensions to the SM, the q-l symmetric model predicts a heavy extra neutral gauge boson, the Z′. The relevant neutral current part of the covariant derivative is

$$D^\mu_{\text{n.c.}} = \partial^\mu + i\frac{g_2}{2}W^\mu_3 \tau_3 + i\frac{g'}{2}C^\mu X + i\frac{g_s}{2\sqrt{3}}G^\mu_8 T, \tag{13}$$

where once again $T = \mathrm{diag}(-2,1,1)$. Defining the VEVs[2] $\langle\phi\rangle \equiv u$ and $\langle\chi_1\rangle \equiv w$, the neutral gauge boson mass matrix is

$$M^2 = \begin{pmatrix} g_2^2 u^2/2 & -g_2 g' u^2/2 & 0 \\ -g_2 g' u^2/2 & g'^2 u^2/2 + 2g'^2 w^2/9 & -2\sqrt{3} g' g_s w^2/9 \\ 0 & -2\sqrt{3} g' g_s w^2/9 & 2g_s^2 w^2/3 \end{pmatrix}. \tag{14}$$

Solving the eigenvalue problem gives

[2]For simplicity, we will write subsequent equations for the case where only one electroweak Higgs doublet is introduced. The generalization to the realistic two-doublet situation does not affect any of the phenomenology we consider in the rest of this paper.

$$M_\gamma^2 = 0,$$
$$M_{Z'}^2 = u^2\kappa_1 + w^2\kappa_2 \mp \sqrt{(u^2\kappa_1 + w^2\kappa_2)^2 - u^2w^2\kappa_3}, \tag{15}$$

where the minus (plus) sign corresponds to the Z (Z′) and

$$\kappa_1 = \frac{1}{4}(g_2^2 + g'^2),$$
$$\kappa_2 = \frac{1}{9}(g'^2 + 3g_s^2), \tag{16}$$
$$\kappa_3 = \frac{1}{9}(g_2^2 g'^2 + 3g_2^2 g_s^2 + 3g'^2 g_s^2).$$

The SM couplings are related to the q-l symmetric couplings by

$$\sin^2(\theta_W)_{\rm SM} \equiv \frac{e^2}{g_2^2} = \frac{g'^2 g_s^2}{3\kappa_3},$$
$$g'^2_{\rm SM} \equiv \frac{e^2}{\cos^2(\theta_W)_{\rm SM}} = \frac{g'^2 g_s^2}{3\kappa_2}. \tag{17}$$

Furthermore, we have

$$u^2 = \frac{2M_W^2}{g_2^2}, \qquad w^2 = \frac{g_2^2}{2\kappa_3}\frac{M_Z^2 M_{Z'}^2}{M_W^2}. \tag{18}$$

The neutral current covariant derivative (13) is rewritten in the gauge-boson mass eigenstate basis as

$$D^\mu_{\rm n.c.} = \partial^\mu + iQ_\gamma A^\mu + iQ_Z Z^\mu + iQ_{Z'} Z'^\mu, \tag{19}$$

where Q_γ, Q_Z and $Q_{Z'}$ are the charges that couple to A^μ, Z^μ and Z'^μ, respectively. The charges coupling to Z and Z′ are given by

$$Q_{Z'} = \pm\left(\frac{\sin^2(\theta_W)_{\rm SM}}{{g'_{\rm SM}}^2} + \frac{1}{4\kappa_1}\left[\eta_{Z'}^2 - \frac{g'^4}{9\kappa_3}\right]\right)^{-1/2} \times \begin{pmatrix} \frac{\tau_3}{2} - \left(\sin^2(\theta_W)_{\rm SM} - \frac{g_2^2 g'^2}{12\kappa_1\sqrt{\kappa_3}}\left[\eta_{Z'}^Z - \frac{g'^2}{3\sqrt{\kappa_3}}\right]\right)Q \\ -\left(\frac{\sqrt{\kappa_3}}{8\kappa_1}\left[\eta_{Z'}^Z - \frac{g'^2}{3\sqrt{\kappa_3}}\right]\right)T \end{pmatrix}, \tag{20}$$

where

$$\eta_{Z'}^Z = \left(\frac{3\sqrt{\kappa_3}}{g'^2} - \frac{6\kappa_1}{g'^2\sqrt{\kappa_3}}\frac{M_Z^2}{w^2}\right)^{-1}. \tag{21}$$

In the $w \to \infty$ limit the quantities within square brackets in Eq. (20) tend to zero for the charge coupling to Z, so that the expression reduces to the SM coupling. To facilitate the calculation of these couplings we write the quantum numbers of the fermions in Table I.

B. Mass limit

A typical signature of a Z′ gauge boson is a high mass resonance in dilepton production through the Drell-Yan process $pp \xrightarrow{Z'} l^+l^-$ [8], in both the dielectron and dimuon channels [9,10]. Recent approaches combine data from each channel to obtain a stronger bound than is possible with a single channel [10].

The aim now is to use LHC data to put a constraint on the mass of the q-l symmetric Z′, henceforth called Z'_{ql}. We achieve this by calculating the cross section $\sigma(pp \xrightarrow{Z'} l^+l^-)$, where l can be either μ or e. As a comparison we also carry out this calculation for the benchmark model of a Z′ with SM coupling, henceforth called $Z'_{\rm SM}$.

We start with the Z′ interaction Lagrangian,

$$\mathcal{L}_{Z'} = \bar{f}\gamma_\mu(g_V'^f - g_A'^f\gamma_5)fZ'^\mu, \tag{22}$$

where

$$g_V'^f = \frac{1}{2}Q_{Z'}(f_L) + \frac{1}{2}Q_{Z'}(f_R),$$
$$g_A'^f = \frac{1}{2}Q_{Z'}(f_L) - \frac{1}{2}Q_{Z'}(f_R), \tag{23}$$

and $Q_{Z'}$ is the charge coupling to the Z′ boson.

We use the Drell-Yan cross section,

$$\sigma(pp \to l^+l^-) = \sum_q \int_0^1\int_0^1 dx_1dx_2 \begin{bmatrix} f_{q/p}(x_1,Q^2)f_{\bar{q}/p}(x_2,Q^2) \\ +f_{q/p}(x_2,Q^2)f_{\bar{q}/p}(x_1,Q^2) \end{bmatrix} \times \sigma(q\bar{q} \to l^+l^-; s = x_1x_2S_{\rm beam}), \tag{24}$$

for a pp collision at $\sqrt{S_{\rm beam}} = 7$ TeV. The parton distribution functions (PDFs), $f_{q/p}(x, Q^2)$, are evaluated using the MSTW08 PDF set at $Q^2 = \frac{1}{4}s$ [11]. We then scale the results for next-to-leading order effects using a k-factor of 1.3 [12].

This cross section is dominated by the parton processes $u\bar{u} \to l^+l^-$ and $d\bar{d} \to l^+l^-$. The parton cross sections in the $\sqrt{s} \gg m_q, m_l$ limit are given by

TABLE I. The quantum numbers of the fermions.

	ν_L	ν_R	e_L	e_R	V_{iL}	V_{iR}	E_{iL}	E_{iR}	u_L	u_R	d_L	d_R
T	−2	−2	−2	−2	1	1	1	1	0	0	0	0
Q	0	0	−1	−1	+1/2	+1/2	−1/2	−1/2	+2/3	+2/3	−1/3	−1/3
τ_3	+1	0	−1	0	+1	0	−1	0	+1	0	−1	0

$$\sigma(q\bar{q} \xrightarrow{Z'} l^+ l^-) = \frac{1}{3}\frac{1}{12\pi}\frac{s}{(s - M_{Z'}^2)^2 + M_{Z'}^2\Gamma_{Z'}^2} \times (|g_V^{lq}|^2 + |g_A^{lq}|^2)(|g_V^{ll}|^2 + |g_A^{ll}|^2), \quad (25)$$

where $M_{Z'}$ is the mass of the Z′ boson. The Z′ width is given to a good approximation by

$$\Gamma_{Z'} = 3(\Gamma(Z' \to \nu_e \bar{\nu}_e) + \Gamma(Z' \to e^+ e^-) + \Gamma(Z' \to u\bar{u}) + \Gamma(Z' \to d\bar{d})),$$
$$\Gamma(Z' \to f\bar{f}) = N_c \frac{M_{Z'}}{12\pi}(|g_V^{lf}|^2 + |g_A^{lf}|^2), \quad (26)$$

where N_c is a color factor equal to 1 for leptons and 3 for quarks. For Z'_{ql} we use Eqs. (20) and (23) to find the couplings, while for $Z'_{\rm SM}$ we use the familiar SM couplings.

The results from our calculations are shown in Fig. 1. The lower bounds on the $M_{Z'}$ parameters, listed in Table II, are given by the upper limit on the cross section at the LHC [10]. We use the ATLAS limit, but a similar result is found using the CMS limit. The lower bound of 1820 GeV for $Z'_{\rm SM}$ agrees with that in the literature. The lower bound of 950 GeV for Z'_{ql} is an improvement of 230 GeV on the previous bound [5], and the best bound to date on a q-l symmetric Z′. The bound for Z'_{ql} is smaller than that for $Z'_{\rm SM}$ due to the quarkphobic nature of Z'_{ql}. In fact, $\mathrm{Br}(Z'_{ql} \to \sum q\bar{q})$ is less than 0.5%.

An analogous calculation was performed for the Tevatron using the upper limit on the cross section from D0 [9]. The results are also given in Table II. The LHC bounds already exceed those of the Tevatron. In the coming years, with more data and higher energy collisions, this bound is set to increase significantly if a Z′ is not discovered first.

In our calculations we have assumed that all the liptons are heavier than $\frac{1}{2}M_{Z'}$, so that none of them is a Z′ decay product. As will be shown in the following section, this need not be the case. We merely make the assumption for simplicity, in order not to introduce too many unknown variables. If liptons are present at low enough masses, the Z′ width increases and the lower bound falls. As an example, for the case of a single left sector lipton of mass 200 GeV, the lower bound on the Z'_{ql} mass from the LHC becomes 930 GeV.

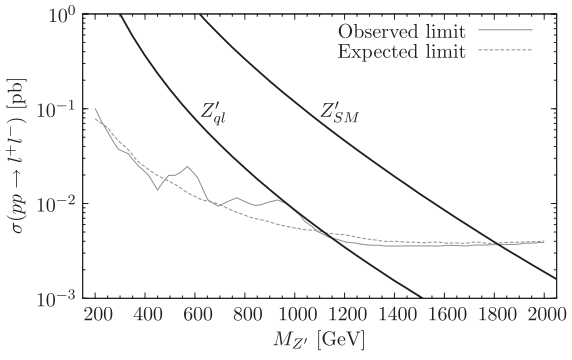

FIG. 1. The cross section $\sigma(pp \to l^+l^-)$ versus $M_{Z'}$ for Z'_{ql} and $Z'_{\rm SM}$. Also shown are the 95% confidence level upper limits on the cross section from ATLAS data [10].

TABLE II. The observed 95% confidence level lower mass limits on $Z'_{\rm SM}$ and Z'_{ql}.

Observed $M_{Z'}$ limit (GeV)		
	Tevatron	LHC
$Z'_{\rm SM}$	1060	1820
Z'_{ql}	780	950

IV. LIPTONS

A. Mass eigenstates

The left and right components of the liptons do not combine to form a Dirac fermion in the obvious way (i.e. $f \neq E_{iL} + E_{iR}$). To understand what actually happens, we need to examine the Lagrangian of Eq. (9); it has the form

$$\mathcal{L}_{\rm mass} = \bar{X}_L \mathcal{M} X_R + \text{H.c.}, \quad (27)$$

where

$$X_L = \begin{pmatrix} V_L \\ (E_R)^c \end{pmatrix}, \qquad X_R = \begin{pmatrix} (E_L)^c \\ V_R \end{pmatrix}, \quad (28)$$

and

$$\mathcal{M} = \begin{pmatrix} m_1 & m_\nu \\ m_e & m_2 \end{pmatrix}. \quad (29)$$

This is for the one-generation case with SU(2)′ indices suppressed. After symmetry breaking, written explicitly, the entries are $m_\nu = \lambda_2 u$, $m_e = \lambda_1 u$ (the usual neutrino and electron mass terms), $m_1 = 2h_1 w$ and $m_2 = h_2^* w$. The nonobservation of liptons implies that the latter two terms are much larger than the former. We assume they are large enough so that the off-diagonal terms can be approximated as zero. In this case we get four exotic Dirac fermions per generation:

$$f_{l1} = (E_{2L})^c + V_{1L}, \qquad f_{l2} = (E_{1L})^c + V_{2L},$$
$$f_{r1} = (E_{2R})^c + V_{1R}, \qquad f_{r2} = (E_{1R})^c + V_{2R}. \quad (30)$$

We call these left (f_{lj}) and right (f_{rj}) sector liptons, with masses m_1 and m_2 respectively. The liptons are degenerate within a sector, each having an SU(2)′ "color" $j = 1, 2$. The conjugation flips the handedness of the spinor, so we always have a left-handed and right-handed part in the Dirac fermion.

Of course, we have little idea of the mass spectrum of these liptons. Our model does not predict the masses, just as the SM does not predict the quark and lepton masses. We

only know that they are massive enough to have not yet been detected.

B. Liptonium

Liptons can be pair produced at the LHC through the Drell-Yan process. The cross section depends primarily on the mass of the liptons and moderately on the mass of the Z′. In the following analysis we focus on the lightest lipton, L. This lipton can be either from the left or the right sector, and we consider both possibilities.

Liptons are charged under the confining SU(2)′ group, so one might think that pair-produced liptons will act like pair-produced heavy quarks. In fact, because there are no light liptons to facilitate SU(2)′ "hadronization," they act very differently. The pair, instead, forms an SU(2)′-neutral bound state, $L\bar{L}$, which we call "liptonium." As we will see, energy is first lost through SU(2)′ glueball radiation. To avoid confusion, and in order to distinguish them from $SU(3)_q$ gluons, we will call the SU(2)′ exotic gluons "huons". Of course, liptons are not charged under $SU(3)_q$ so do not couple to gluons.

Much of our expectations can be inferred from the work of Carlson *et al.* [13], wherein the phenomenology and collider signatures of the color SU(5) model of Foot and Hernandez [14] were studied. This model has the same intermediate and low-energy gauge structure (4) as the q-l symmetric model. The analogy to liptonium in the color SU(5) model is quirkonium, formed from "quirks" which have the same quantum numbers as our liptons. These quirks are doublets under an unbroken group analogous to our SU(2)′ group.

Following Ref. [13], we assume that the invariant mass of the lipton pair is well above the threshold $\sim 2m_L$, but below $4m_L$. The lipton pair can be viewed as a highly excited liptonium state. The deexcitation of this state will occur in two distinct stages.

The first stage is hueball emission. As the liptons oscillate in the potential, many hueballs will be radiated with no preferential direction in the liptonium frame. This will lead to a large amount of missing energy but only a small amount of missing transverse energy. The hueballs will also carry away a significant amount of angular momentum, leaving the liptonium with large J. When the excitation energy drops beneath the hueball mass, deexcitation will occur through photon emission. It is unclear whether these photons will be hard or soft compared to the hueball mass.

The second stage occurs when the liptons enter the one-huon-exchange Coulomb potential

$$V(r) = -3\alpha_s(r)/4r \tag{31}$$

regime. Here we assume that the liptonium has a large orbital quantum number l and that spin states $S = 1$ and $S = 0$ are populated in the ratio 3:1. Annihilation of the liptons to huons is small for high l states, and $|\Delta l| = 1$ electromagnetic transitions are favored. (Spin flip transitions are small and can be ignored.) There will be many of these soft photon emissions until the liptonium is in the n^3P or n^1P state. From here, parity symmetry prevents all lipton pairs annihilating to invisible hueballs. The n^1P states cascade predominantly to n^1S states which annihilate to photons or huons. The n^3P states can annihilate to huons or cascade to n^3S states. The cascade always dominates [13]. The parity symmetry then prevents the n^3S states annihilating entirely to huons, and s-channel neutral current annihilations are expected to dominate.

Thus we expect that approximately 75% of the total pair-produced liptons will eventually reach ^3S states. From here they can annihilate to W^+W^-, Z Higgs, $hh\gamma$, hhZ and $f\bar{f}$, where h are huons. The most exciting products are SM fermions. Production through this mechanism will result in lepton pairs or jets of invariant mass $\sim 2m_L$. Similarly, we expect that approximately 25% of pair-produced liptons will reach ^1S states where they can annihilate to invisible huons or diphotons.

If the decay of liptonium occurs as we expect, then liptons with mass less than ~ 100 GeV are ruled out by the Large Electron-Positron (LEP) collider experiments. This is because LEP, running at up to $\sqrt{S_{\text{beam}}} = 209$ GeV, was able to tag large missing energy events [15]. If $m_L < 100$ GeV then the large missing energy resulting from the first stage of liptonium deexcitation would have been detected at LEP in dilepton events. The LHC experiment does not have this capability, instead only being able to tag large missing transverse energy events.

C. Seeing liptons at the LHC

Our aim now is to determine the cross section $\sigma(pp \to f\bar{f})$ through the liptonium resonance. This cross section can be approximated by

$$\sigma(pp \xrightarrow{L\bar{L}} l^+l^-) \approx \sigma(pp \to L\bar{L}) \times 0.75 \times \text{Br}(^3S_1 \to l^+l^-), \tag{32}$$

where the factor of 0.75 accounts for the fraction of liptonium states which reach the $^3S_1$ state. The $\sigma(pp \to L\bar{L})$ and $\text{Br}(^3S_1 \to l^+l^-)$ factors will be given in the following two subsections.

1. $\sigma(pp \to L\bar{L})$

In our analysis, we ignore the contribution of the Z′ neutral current by taking the limit $w \to \infty$, where $Q_Z = Q_Z^{\text{SM}}$. This will be justified in a moment. We start with the neutral current interaction Lagrangian,

$$\mathcal{L}_{\text{n.c.}} = e\bar{f}\gamma_\mu Q f A^\mu + \bar{f}\gamma_\mu(g_V^f - g_A^f\gamma_5) f Z^\mu. \tag{33}$$

We calculate $\sigma(pp \to L\bar{L})$ using the Drell-Yan cross section (24). The parton cross sections are found in the $\sqrt{s}$, $m_L \gg m_q$ limit using

$$\sigma(q\bar{q} \xrightarrow{\gamma,Z} L\bar{L}) = \frac{2}{3}Q_q^2 Q_L^2 \frac{8\pi\alpha^2}{s^2}\sqrt{1-\frac{4m_L^2}{s}} \times \left\{ \begin{array}{c} (1 + 2\mathrm{Re}(\chi) g_V^q g_V^L)\left[\frac{1}{6}s + \frac{1}{3}m_L^2\right] \\ +|\chi|^2\left\{ \begin{array}{c} (|g_V^q|^2 + |g_A^q|^2)(|g_V^L|^2 + |g_A^L|^2)\left[\frac{1}{6}s - \frac{1}{6}m_L^2\right] \\ +\frac{1}{2}(|g_V^q|^2 + |g_A^q|^2)(|g_V^L|^2 - |g_A^L|^2)m_L^2 \end{array} \right\} \end{array} \right\}, \tag{34}$$

where

$$\chi = \frac{1}{4\pi Q_q Q_L \alpha}\frac{s}{(s - M_Z^2 + iM_Z\Gamma_Z)}. \tag{35}$$

The χ-independent term is the pure photon contribution, the $|\chi|^2$ term is the pure Z contribution, and the $\mathrm{Re}(\chi)$ term is the γ/Z interference term. The width, Γ_Z, is given by equations analogous to (26).

To justify ignoring the Z′ contribution, we consider the ratio

$$R = \sigma(q\bar{q} \xrightarrow{Z'} L\bar{L})/\sigma(q\bar{q} \xrightarrow{\gamma,Z} L\bar{L}) \tag{36}$$

as a function of Z′ mass. The quantity $\sigma(q\bar{q} \xrightarrow{Z'} L\bar{L})$ is found analogously to the pure Z contribution in Eq. (34), with the width of Z′ modified to include decay to a single family of lightest liptons when $M_{Z'} > 2m_L$. We find that R is largest for left (right) sector liptons when $M_{Z'} \approx 2.5m_L$, where $R \approx 0.12$ ($R \approx 0.56$). Away from this resonance the contribution is much smaller, and given that $M_{Z'} > 950$ GeV this coincidence is unlikely in the region that will be of interest.

2. $\mathbf{Br}(^3S_1 \to l^+l^-)$

The decay rate of the $^3S_1$ liptonium state to a pair of fermions is given by the spin- and color-summed squared matrix element multiplied by the square of the liptonium wave function at the origin [16]. In the $m_f \to 0$ limit, we find

$$\Gamma(^3S_1 \to f\bar{f}) = N_c Q_f^2 \frac{2\pi\alpha^2}{3m_L^2}|\Psi(0)|^2\left[\begin{array}{c} (1 + 2\mathrm{Re}(\chi_0) g_V^L g_V^f) \\ +|\chi_0|^2(|g_V^L|^2 + |g_A^L|^2)(|g_V^f|^2 + |g_A^f|^2) \end{array} \right], \tag{37}$$

where $\chi_0 := \chi|_{s=4m_L^2}$ with χ given by Eq. (35) [with Q_q replaced by Q_f]. This expression is appropriate for all fermions except for the especially heavy top quark. For the top quark, we find

$$\Gamma(^3S_1 \to t\bar{t}) = \frac{8\pi\alpha^2}{9m_L^2}|\Psi(0)|^2\sqrt{1-\frac{m_t^2}{m_L^2}} \times \left[\begin{array}{c} (1 + 2\mathrm{Re}(\chi_0) g_V^L g_V^t)\left(1 + \frac{m_t^2}{2m_L^2}\right) \\ +|\chi_0|^2(|g_V^L|^2 + |g_A^L|^2)(|g_V^t|^2 + |g_A^t|^2)\left(1 - \frac{m_t^2}{4m_L^2}\right) \end{array} \right]. \tag{38}$$

In our analysis, the W^+W^-, Z Higgs, $hh\gamma$ and hhZ decay channels of the $^3S_1$ state are ignored. For lipton masses greater than 100 GeV, they each contribute of order 2% [13]. We take the total decay rate as

$$\begin{aligned}\Gamma(^3S_1) = {} & 2\Gamma(^3S_1 \to u\bar{u}) + \Gamma(^3S_1 \to t\bar{t}) + 3\Gamma(^3S_1 \to d\bar{d}) \\ & + 3\Gamma(^3S_1 \to e^+e^-) + 3\Gamma(^3S_1 \to \nu_e\overline{\nu_e})\end{aligned} \tag{39}$$

and use Eqs. (37) and (38) to find the branching fractions. The results are shown in Fig. 2. We include the experimentally excluded region, $m_L < 100$ GeV, so that the interested reader may compare the results with those for the color SU(5) model [13].

3. Cross section

The cross section of two hadrons to a single lepton pair via the liptonium channel can now be found using Eq. (32). The resulting cross sections for the LHC are shown in Fig. 3.

4. $^3S_1$ width

The vertical axis of Fig. 3 can be read as "the number of events per 1 fb^{-1} of integrated luminosity in the dilepton channel," where "dilepton" could either mean dielectron or dimuon. Given enough data, these events would be detected as a peak in the dilepton invariant mass spectrum at $m_{ll} \sim 2m_L$. We would like to have some idea of the width of this peak. To achieve this, we must evaluate Eq. (39).

With the liptonium in the one-huon-exchange potential (31) regime, standard results for hydrogenic wave functions tell us that, with fixed $\alpha_s(r) = \alpha_s(m_L)$, we have

$$|\Psi_n(0)|^2 = \left(\frac{3}{8}n^{-1}m_L\alpha_S(m_L)\right)^3/\pi, \tag{40}$$

where n is the radial quantum number. For $n = 1$ and m_L varying from 100–600 GeV, $\Gamma(^3S_1)$ varies from ~1–100 keV.

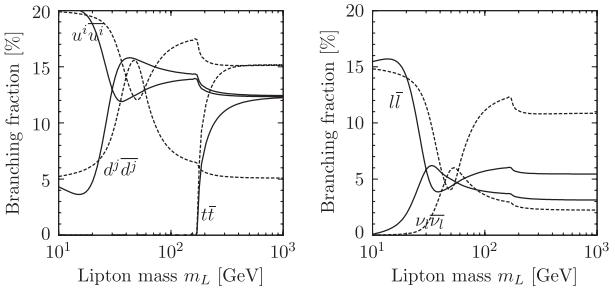

FIG. 2. Branching fractions of the ${}^3S_1$ liptonium state to difermions. The solid (dashed) lines correspond to left (right) sector liptons and $i = \{1, 2\}$, $j = \{1, 2, 3\}$ are family indices.

The energy resolution of the ATLAS electromagnetic liquid argon calorimeter is $\sigma(E)/E = 10\%/\sqrt{E(\mathrm{GeV})} + 0.7\%$ [17]. The detector sees a convolution of the true peak and the Gaussian defined by variance $\sigma^2(E)$. Since the resolution is much larger than the width of the liptonium invariant mass peak, we can assume that the observed peak is a Gaussian with 68% of events in the window of width $2\sigma(E)$ surrounding the peak energy $2m_L$.

5. Seeing liptons

We now make an estimate for the amount of data needed to see a liptonium resonance in the dilepton channel. For an invariant mass of m_{ll} we employ a bin width of $2\sigma(m_{ll})$. We then compare the number of background events, N_b, with the number of signal events, N_s, in this bin.

The number of background events in the dimuon and dielectron channels is determined by extrapolating the number of SM events expected in an ATLAS dilepton resonance search [10] using

$$N = \sigma \int \mathcal{L} dt, \tag{41}$$

where $\int \mathcal{L} dt$ is the integrated luminosity.

The number of signal events is given by $N_s = \mathcal{A} \times \sigma(pp \xrightarrow{L\bar{L}} l^+ l^-) \int \mathcal{L} dt$, where $\mathcal{A}$ is the acceptance for the signal assuming the same analysis cuts as in Ref. [10]. The typical value for a spin-1 resonance with these cuts is $\mathcal{A} \approx 0.65$ ($\mathcal{A} \approx 0.40$) in the dielectron (dimuon) channel.

The number of observed background events fluctuates according to a Poisson distribution with a standard deviation of $\sqrt{N_b}$. If we know the number of background and the number of signal events for 1 fb^{-1} of data, n_b and n_s, we can extrapolate to the number of events in x fb^{-1} of data using Eq. (41): xn_b and xn_s. The point where the signal reaches 3σ significance inside the window, or when $N_s = 3\sqrt{N_b}$, is at

$$x = \frac{9n_b}{n_s^2}. \tag{42}$$

This is the point at which the liptonium resonance is noticeable.

The results versus lipton mass are shown in Fig. 4. Also shown in Fig. 4 are the cases of the closely related SU(5) and SU(7) leptonic color models [18]. The cross section to diliptons is proportional to a color factor $N - 1$ for SU(N) leptonic color, so, compared to the SU(3) leptonic color model, the amount of integrated luminosity needed for 3σ signal significance decreases by $1/4$ and $1/9$ for SU(5) and SU(7), respectively.

These calculations have been carried out for the LHC running at 7 TeV. They can readily be recalculated for the LHC at 14 TeV following a similar procedure. We stress that this analysis is simplified and could be improved with smarter analysis cuts. Our results illustrate that in the foreseeable future, with the LHC set to gather more than 100 fb^{-1} of data, the LHC will explore lipton mass parameter space beyond 100 GeV, an improvement on the LEP frontier.

A similar calculation for the diphoton product of the liptonium ${}^1S$ state shows that we need $\sim 10^6$ fb^{-1} to see a 100 GeV liptonium resonance at 3σ significance. A liptonium dilepton resonance will therefore present itself with

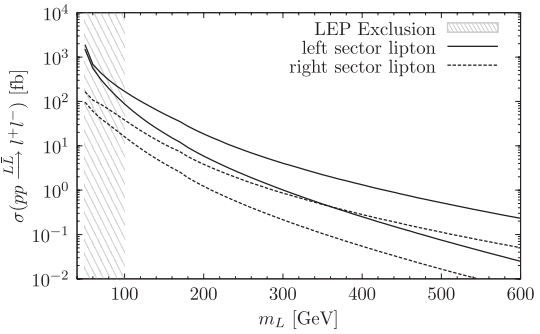

FIG. 3. Cross section of $pp \to l^+ l^-$ through the production of liptonium and the subsequent decay of the ${}^3S_1$ state for the LHC at 14 TeV and 7 TeV descending.

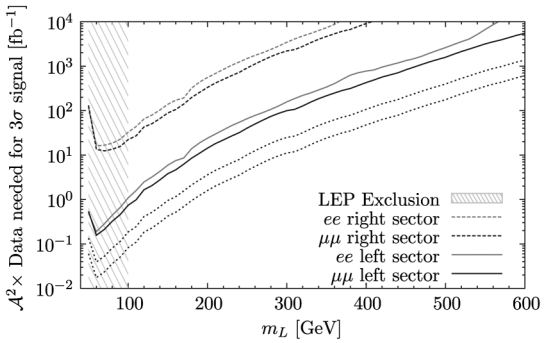

FIG. 4. The amount of data in fb^{-1} we need to see a liptonium resonance at 3σ significance multiplied by the acceptance squared. [For $m\sigma$ significance multiply by a factor $m^2/9$]. The dotted grey lines are for dimuon channel left sector liptons with SU(5) or SU(7) leptonic color descending.

the absence of such a resonance in the diphoton channel. This is one way of discerning the resonance from other particles such as the Randall-Sundrum graviton [19].

V. COLOR TRIPLET DIQUARK

We will now focus on the phenomenology of the Higgs scalars contained within the Yukawa Lagrangian (9). We are interested in signatures at the LHC, so we concentrate on the QCD coloured scalar χ_2, a color triplet diquark. Diquarks are generically predicted by a number of bottom-up models and GUTs, and are well studied in the literature [see e.g. Ref. [20]].

A. Constraints

Rewriting the χ_2 Lagrangian with generational indices, we have

$$\mathcal{L} = 2(h_1)_{ij}\overline{(u_L^i)^c}d_L^j\chi_2 + (h_2)_{ij}\overline{(u_R^i)^c}d_R^j\chi_2 + \text{H.c.} \quad (43)$$

Color asymmetry and asymmetry in the SU(2) contraction implies that h_1 is symmetric in flavour space when the quarks are in the gauge basis. Flavour rotation to the mass basis does not retain this symmetry, because distinct rotations must be applied to u_L and d_L. There is no symmetry/antisymmetry condition on the h_2 matrix.

The χ_2 diquark transforms as (3, 1) under $\mathrm{SU}(3)_q \times \mathrm{SU}(2)_L$. If one considers only these SM charges then the scalar can also behave as a leptoquark through the terms $\overline{(f_L)^c}q_L\bar{\chi}$ and $\overline{(e_R)^c}u_R\bar{\chi}$. These terms lead to rapid decay of the proton through tree-level exchange unless the mass of the scalar is very large, so they need to be forbidden if we are to have any chance of seeing this scalar at the LHC. The usual mechanism is baryon parity [20] or U(1) symmetry [21]. The q-l symmetric model provides a natural mechanism. If one tries to write down the terms $\overline{(F_L)^c}Q_L\bar{\chi}$ and $\overline{(u_R)^c}E_R\bar{\chi}$ it quickly becomes clear that they are not gauge invariant unless χ transforms as a 3 under both $\mathrm{SU}(3)_q$ and $\mathrm{SU}(3)_l$. So this χ cannot be our χ_2. Further, if we tried to replace χ_2 with such a χ [transforming like (3, 3, 1)] the terms $\overline{(Q_L)^c}Q_L\chi_2$ and $\overline{(u_R)^c}d_R\chi_2$ would not be gauge invariant under $\mathrm{SU}(3)_l$. So, q-l symmetry naturally forbids the leptoquark terms. Thus, there are no constraints on χ_2 from proton decay.

We must also suppress flavor changing neutral currents to avoid strong constraints from meson-antimeson mass mixing measurements. To achieve this we must adopt for h_1 and h_2 a suitable Yukawa-coupling ansatz. It will be sufficient for us to define the h_1 and h_2 matrices diagonally in the mass basis, as in Ref. [22]. In this way, we avoid flavor changing neutral current concerns.

B. Cross section

We now turn to phenomenology at hadron colliders. If we restrict ourselves to considering proton valence quarks, with a diagonal Yukawa-coupling ansatz we are considering only three parton-level processes: the s-channel processes $ud \to ud$, cs, tb. The first two processes result in a dijet final state, while the last is a single top + b-jet. The single top signal is the preferred method for a χ_2 diquark search at the LHC due to a lower SM background [23]. The s-channel process mediated by χ_2 and producing a single top is shown in Fig. 5.

Our goal is to calculate $\sigma(pp \xrightarrow{\bar{\chi}_2} tb)$ as a function of χ_2 mass and couplings. To facilitate our calculation, we write the Lagrangian in the Dirac basis:

$$\mathcal{L} = \overline{(u^i)^c}[(g_V)_{ij} - (g_A)_{ij}\gamma_5]d^j\chi_2 + \text{H.c.}, \quad (44)$$

where

$$\begin{aligned}(g_V)_{ij} &= \frac{1}{2}[2(h_1)_{ij} + (h_2)_{ij}],\\ (g_A)_{ij} &= \frac{1}{2}[2(h_1)_{ij} - (h_2)_{ij}].\end{aligned} \quad (45)$$

Because h_1 and h_2 are diagonal, g_V and g_A are also diagonal.

The dominant parton-level process is $ud \xrightarrow{\bar{\chi}_2} tb$. The cross section in the $m_{u,d,b} \ll m_t$ limit is

$$\begin{aligned}\sigma(ud \xrightarrow{\bar{\chi}_2} tb) = \frac{1}{12\pi}\left(\frac{s-m_t^2}{s}\right)^2 \frac{s}{(s-M_\chi^2)^2 + M_\chi^2\Gamma_\chi^2}\\ \times(|(g_V)_{11}|^2 + |(g_A)_{11}|^2)(|(g_V)_{33}|^2 + |(g_A)_{33}|^2),\end{aligned} \quad (46)$$

where M_χ, Γ_χ are the mass and width of χ_2. The full width is given by the sum of partial widths

$$\begin{aligned}\Gamma(\bar{\chi}_2 \to u^{i=[1,2]}d^j) &= \frac{M_\chi}{4\pi}(|(g_V)_{ij}|^2 + |(g_A)_{ij}|^2),\\ \Gamma(\bar{\chi}_2 \to td^j) &= \frac{M_\chi}{4\pi}\left(1 - \frac{m_t^2}{M_\chi^2}\right)^2(|(g_V)_{3j}|^2 + |(g_A)_{3j}|^2).\end{aligned} \quad (47)$$

The cross section at a hadron collider is expressed in terms of PDFs in a similar way to the Drell-Yan process (24):

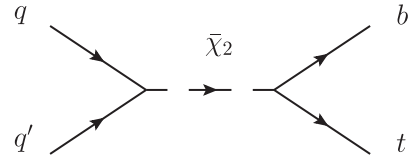

FIG. 5. Single top production mediated by the χ_2 diquark.

$$\sigma(pp\xrightarrow{\bar{\chi}_2}tb)$$
$$= \sum_{i,j}\int_0^1\int_0^1 dx_1 dx_2 \begin{bmatrix} f_{u^i/p}(x_1,Q^2) f_{d^j/p}(x_2,Q^2) \\ +f_{u^i/p}(x_2,Q^2) f_{d^j/p}(x_1,Q^2) \end{bmatrix}$$
$$\times \sigma(u^i d^j \xrightarrow{\bar{\chi}_2} tb; s = x_1 x_2 S_{\text{beam}}). \quad (48)$$

The cross section $\sigma(pp\xrightarrow{\chi_2}\bar{t}\,\bar{b})$ is found similarly. At the LHC, top-quark production is preferred over antitop production due to nonzero initial baryon number, so that $\sigma(pp\xrightarrow{\bar{\chi}_2}tb) \gg \sigma(pp\xrightarrow{\chi_2}\bar{t}\,\bar{b})$. The case for the Tevatron is different, with $\sigma(p\bar{p}\xrightarrow{\bar{\chi}_2}tb) = \sigma(p\bar{p}\xrightarrow{\chi_2}\bar{t}\,\bar{b})$.

The parton-level cross section in Eq. (48) will have a distinct peak at $x_1 x_2 S_{\text{beam}} = M_\chi^2$. The height and width of this peak is determined by the χ_2 width (47), which can be quite small depending on the coupling. This causes numerical problems when integrating Eq. (48) directly. It is convenient instead to introduce a change of variable, $x_2 = M_{\text{inv}}^2/x_1 S_{\text{beam}}$, so that the peak is only dependent on one integration variable: the invariant mass of tb, M_{inv}. Making this substitution, and only considering valence quarks at the parton-level, we obtain

$$\frac{d\sigma(pp\xrightarrow{\bar{\chi}_2}tb)}{dM_{\text{inv}}} = \int_{(M_{\text{inv}}^2/S_{\text{beam}})}^1 dx \frac{2M_{\text{inv}}}{xS_{\text{beam}}} \times \begin{bmatrix} f_{u/p}(x,Q^2) f_{d/p}\left(\frac{M_{\text{inv}}^2}{xS_{\text{beam}}},Q^2\right) \\ +f_{u/p}\left(\frac{M_{\text{inv}}^2}{xS_{\text{beam}}},Q^2\right) f_{d/p}(x,Q^2) \end{bmatrix}$$
$$\times \sigma(ud\xrightarrow{\bar{\chi}_2}tb; s = M_{\text{inv}}^2). \quad (49)$$

One may then find the total cross section by integrating over the invariant mass. The total integration is over $M_{\text{inv}} = (0, \sqrt{S_{\text{beam}}})$, with the region near $M_{\text{inv}} = M_\chi$ dominating the cross section.

C. Mass/coupling limits

A Bayesian approach to calculating and combining CDF and D0 Tevatron results for the single top cross section is presented in Ref. [24]. The quantity includes both s-channel and t-channel contributions to single top and single anti-top quark final states. (In the language of hadron colliders, ''single top'' means single top quark or single anti-top quark.) The single top cross section is found to be

$$\sigma^{\text{Tevatron}}_{(s+t)-ch}(p\bar{p}\to tX;\bar{t}X) = 2.76^{+0.56}_{-0.47}\ \text{pb} \quad (50)$$

for a 170 GeV top quark. This is in good agreement with the SM theoretical prediction of $3.33^{+0.08}_{-0.10}$ pb [25]. We can use this measurement to put a limit on the cross section of our diquark mediated process. A conservative bound is

$$\sigma^{\text{Tevatron}}(p\bar{p}\to tb;\bar{t}\,\bar{b}) < 1\ \text{pb}. \quad (51)$$

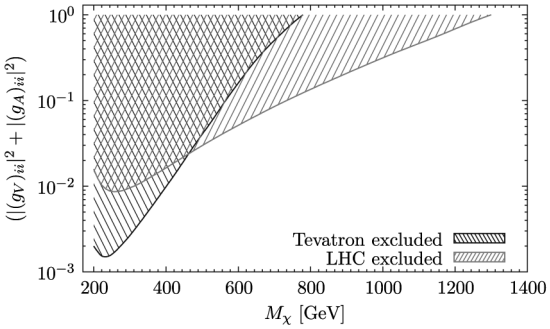

FIG. 6. The experimentally excluded regions of χ_2 parameter space.

For the LHC at 7 TeV, the SM theoretical prediction for the single top s-channel cross section is ~4.6 pb [25]. There is not yet enough data to statistically observe single top production in this channel. However, the preliminary limit [26],

$$\sigma^{\text{LHC@7TeV}}_{s-ch}(pp\to tX;\bar{t}X) < 26.5\ \text{pb}, \quad (52)$$

is enough to compete with Tevatron bounds, as we will see.

We calculated $\sigma(pp\to tb;\bar{t}\,\bar{b})$ and $\sigma(p\bar{p}\to tb;\bar{t}\,\bar{b})$ as a function of M_χ and $(|(g_V)_{ii}|^2 + |(g_A)_{ii}|^2)$ using Eq. (49). Here we made no assumptions on the magnitude relationship between entries of the generational matrices h_1 and h_2. PDFs were evaluated using the MSTW08 PDF set at $Q^2 = \frac{1}{4}s$. A k-factor of 1.3 was used for both the Tevatron and LHC calculations [27]. We then used Eqs. (51) and (52) to put constraints on the two dimensional mass-coupling space. Our results are shown in Fig. 6. We see that the LHC can already impose bounds that exceed those of the Tevatron at sufficiently large coupling.

VI. CONCLUSION

We have studied the phenomenology of the quark-lepton symmetric model of Foot and Lew [1] in the context of the LHC. In this model, an $SU(3)_l$ ''leptonic color'' symmetry is appended to the SM gauge group, tripling the number of SM leptons. Consequently, a Z_2 discrete quark-lepton symmetry of the Lagrangian can be defined. The additional symmetries are then spontaneously broken by an $SU(3)_l$ triplet Higgs multiplet, the Z_2 partner of which is an $SU(3)_q$ triplet diquark called χ_2. After this breaking, the eight gauge bosons of $SU(3)_l$ become a heavy neutral Z' gauge boson [in conjunction with the gauge boson of $U(1)_X$], three massless exotic gluons (huons) mediating an unbroken confining $SU(2)'$ force, and four charge $\pm 1/2$ ''weak'' bosons [these four bosons do not couple to quarks and are not expected to exhibit prominent LHC phenomenology]. There are also four massive $\pm 1/2$ charged exotic leptons (liptons) per family which transform as doublets under $SU(2)'$. The SM particles are uncharged under $SU(2)'$.

We investigated three main areas of interest at the LHC: the Z' heavy neutral gauge boson, the liptons, and the diquark χ_2.

Using dilepton data, we put lower bounds on the mass of the Z' gauge boson of 780 GeV and 950 GeV, from the Tevatron and LHC, respectively. The latter is an improvement of 230 GeV on the previous best limit [5].

We then considered lipton pair production, $L\bar{L}$, at the LHC through the Drell-Yan mechanism. All pairs form excited ''liptonium'' bound states. These states then deexcite via isotropic hueball and soft photon radiation, resulting in large missing energy. It was estimated that 75% of liptonium states will annihilate to difermions while 25% annihilate to diphotons and huons. The diphoton events were found to be too few in number to detect at the LHC. However, we found that annihilation to dileptons will be observable at the LHC in the near future for lipton mass $m_L > 100$ GeV, the current bound set by the LEP experiments. New lipton mass parameter space is already being explored by the LHC for the closely related SU(5) and SU(7) leptonic color models.

Last, we investigated the phenomenology of the color triplet scalar diquark χ_2. Using single top production data from the Tevatron and LHC we excluded areas of the two dimensional mass-coupling parameter space, as shown in Fig. 6. We found that the LHC is already competitive with Tevatron bounds.

ACKNOWLEDGMENTS

This work was supported in part by the Australian Research Council.

[1] R. Foot and H. Lew, Phys. Rev. D **41**, 3502 (1990).
[2] J. C. Pati and A. Salam, Phys. Rev. D **10**, 275 (1974).
[3] G. Senjanovic and R. N. Mohapatra, Phys. Rev. D **12**, 1502 (1975).
[4] G. C. Joshi and R. R. Volkas, Phys. Rev. D **45**, 1711 (1992); K. Babu, E. Ma, and S. Willen-brock, *ibid.* **69**, 051301 (2004); S.-L. Chen and E. Ma, Mod. Phys. Lett. A **19**, 1267 (2004); A. Demaria, C. I. Low, and R. R. Volkas, Phys. Rev. D **72**, 075007 (2005); **73**, 079902(E) (2006); **74**, 033005 (2006); A. Demaria and K. L. McDonald, *ibid.* **75**, 056006 (2007); K. Babu, T. W. Kephart, and H. Pas, *ibid.* **77**, 116006 (2008); D. A. Eby, P. H. Frampton, X.-G. He, and T. W. Kephart, *ibid.* **84**, 037302 (2011).
[5] R. Foot, H. Lew, and R. R. Volkas, Phys. Rev. D **44**, 1531 (1991).
[6] Y. Levin and R. R. Volkas, Phys. Rev. D **48**, 5342 (1993).
[7] R. Foot and R. R. Volkas, Phys. Lett. B **358**, 318 (1995).
[8] S. D. Drell and T.-M. Yan, Ann. Phys. (N.Y.) **66**, 578 (1971).
[9] T. Aaltonen *et al.* (CDF Collaboration), Phys. Rev. Lett. **106**, 121801 (2011); V. M. Abazov *et al.* (D0 Collaboration), Phys. Lett. B **695**, 88 (2011).
[10] G. Aad *et al.* (ATLAS Collaboration), Phys. Rev. Lett. **107**, 272002 (2011); V. Timciuc (CMS Collaboration), arXiv:1111.4528.
[11] A. D. Martin, W. J. Stirling, R. S. Thorne, and G. Watt, Eur. Phys. J. C **63**, 189 (2009).
[12] R. Hamberg, W. L. van Neerven, and T. Matsuura, Nucl. Phys. B **359**, 343 (1991); **644**, 403(E) (2002); V. Khachatryan *et al.* (CMS Collaboration), Phys. Lett. B **698**, 21 (2011).
[13] E. D. Carlson, L. J. Hall, U. Sarid, and J. W. Burton, Phys. Rev. D **44**, 1555 (1991).
[14] R. Foot and O. F. Hernandez, Phys. Rev. D **41**, 2283 (1990).
[15] P. Achard *et al.* (L3 Collaboration), Phys. Lett. B **587**, 16 (2004).
[16] T. Appelquist and H. D. Politzer, Phys. Rev. D **12**, 1404 (1975).
[17] M. Aurousseau (ATLAS LAr), Nucl. Phys. B, Proc. Suppl. **215**, 110 (2011).
[18] R. Foot and R. R. Volkas, Phys. Lett. B **645**, 345 (2007).
[19] S. Chatrchyan *et al.* (CMS Collaboration), arXiv:1112.0688; ATLAS Collaboration, arXiv:1112.2194.
[20] G. F. Giudice, B. Gripaios, and R. Sundrum, J. High Energy Phys. 08 (2011) 055.
[21] M. A. Ajaib, I. Gogoladze, Y. Mimura, and Q. Shafi, Phys. Rev. D **80**, 125026 (2009).
[22] I. Gogoladze, Y. Mimura, N. Okada, and Q. Shafi, Phys. Lett. B **686**, 233 (2010).
[23] S. Chatrchyan *et al.* (CMS Collaboration), Phys. Lett. B **704**, 123 (2011); G. Aad *et al.* (ATLAS Collaboration), Phys. Lett. B **708**, 37 (2012).
[24] A. Heinson and T. R. Junk, Annu. Rev. Nucl. Part. Sci. **61**, 171 (2011).
[25] N. Kidonakis, Phys. Rev. D **81**, 054028 (2010); **83**, 091503 (2011).
[26] Search for s-channel single top-quark production in pp collisions at $\sqrt{s} = 7$ TeV, CERN, Tech. Rep. No. ATLAS-CONF-2011-118, Geneva, 2011.
[27] T. Han, I. Lewis, and T. McElmurry, J. High Energy Phys. 01 (2010) 123.